Simulation of the Destruction Effects in CMOS-Devices caused by Impact of Fast Transient Electromagnetic Pulses

M. Rohe*, S. Korte, M. Koch
Leibniz Universität Hannover – Institute for the Basics of Electrical Engineering and Measurement Science
*Appelstraße 9A, 30167 Hannover, RoheMel@aol.com

Abstract: In this paper will be presented how an electronic system and its components will respond in case of an impact of an external electromagnetic pulse (EMP). In the first instance the coupling process of transient electromagnetic pulses into electronic systems will be shown. Out of that the disturbing signal inside the system, which is necessary for the following simulation, will be described analytically. Furthermore, the microscopical analysis of the occuring destruction effects will be shown. The theory of the multiphysics simulation, which connects the heat transfer and electrostatics modules, will be discussed in detail. Against this background, simulations of different destruction effects will be shown in comparison to the microscopical analysis. The gain in new information about the destruction processes will be discussed.

Keywords: pulse, EMP, coupling, destruction, CMOS, electrothermal

1. Introduction

Over the past few years the use of electronics, its components and assemblies is constantly increased. Evidently, there is a risk of generating disturbing signals inside the electronic system by injection of external electromagnetic fields. A breakdown or destruction of electronic systems would be inconceivable and devastating. Nowadays, it is practicable to generate transient ultrawideband pulses (UWB) with a high amplitude and very short rise times. As a radiated electromagnetic field these pulses have an effect on the function of modern electronics.

2. Coupling Process

In order to analyse the coupling process of electromagnetic pulses into electronic systems so-called TEM-Waveguides are used. Transversal electromagnetic waves propagate in the TEM-Waveguide, which could be described as a widened segment of a coaxial transmission line. The test area inside the waveguide is large enough to position a test setup of electronic circuits. Combined with different pulse generators, the TEM-Waveguide allows to generate reproducible transient electromagnetic pulses with a defined field strength and pulse form.
The characteristic of a double-exponential pulse is shown in Figure 1. Three variables describe the pulse form of a double-exponential pulse: E_0 characterizes the amplitude of the electric field, t_r describes the rise time and t_{fwhm} the full width at half maximum, which characterizes the pulse duration. The rise time and pulse length are determined by the source (cp. Table 1).

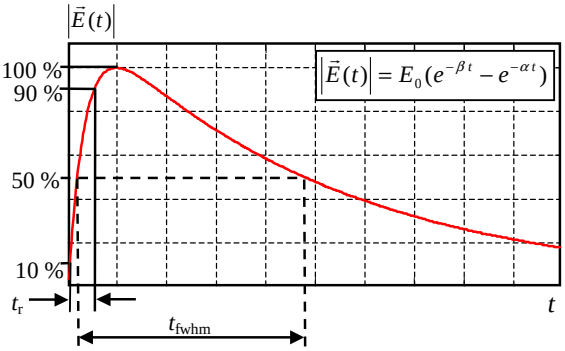

Figure 1. Double-exponential pulse

Source	Risetime t_r	Pulse length t_{fwhm}
UWB (artificial)	< 100ps	> 1ns
NEMP (nuclear electromagnetic pulse)	1ns – 5ns	> 100ns
LEMP (lightning)	1ms – 2ms	>> 50ms

Table 1 Pulse characteristics

The spectra of the different pulse forms are shown in Figure 2. The energy content at high frequencies increases with decreasing pulse duration and rise time.
In order to analyse the coupling process of an electronic system it is necessary to define the transfer function of the coupling process:

$$G(j\omega) = \frac{U_E(j\omega)}{E(j\omega)} \quad . \qquad (1)$$

This function results from the external electric field $E(j\omega)$, which is applied to the electronic system, and the coupled-in voltage $U_E(j\omega)$. Figure 3 shows such a transfer function of a system with a line length of l = 20 cm between the system components.

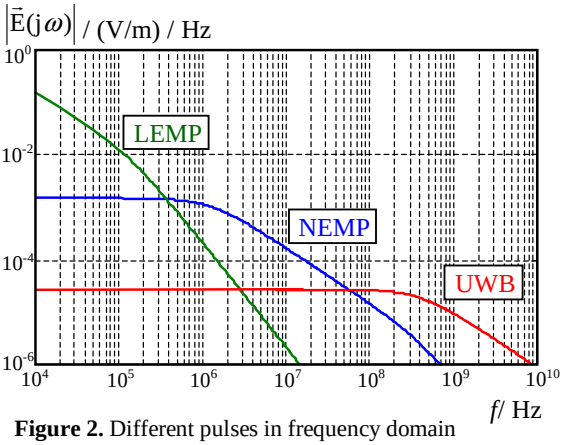

Figure 2. Different pulses in frequency domain

Noticeable is a frequency domain between f_1 and f_2 , where a large part of the energy couples into system. Below the frequency f_1 and above the frequency f_2 the coupling into the system is negligible. The two critical frequencies are defined by the dimensions of the system [1, 2]. The typical coupling frequencies of electronic systems lie between several 10 MHz and a few GHz [3].
In comparison of Figures 2 and 3, a specific characteristic of ultra-wideband pulses becomes apparent. UWB-pulses are able to disturb electronic systems with a much lower amplitude than other pulse forms, based on the facts that its spectrum has more content in the coupling range of the system.

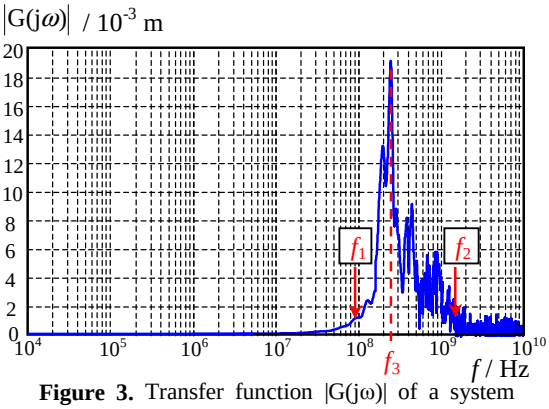

Figure 3. Transfer function |G(jω)| of a system with a line length of l = 20 cm

Basically, the disturbing signal couples into an electronic system via connecting lines and printed circuit board tracks. A direct coupling into chips occurs at much higher frequencies and high amplitudes because the dimensions of the integrated devices are very short (nm-range). Against this background the following surveys only consider coupling processes through connecting lines.
The investigations presented in this paper are carried out with the field pulse shown in Figure 4.

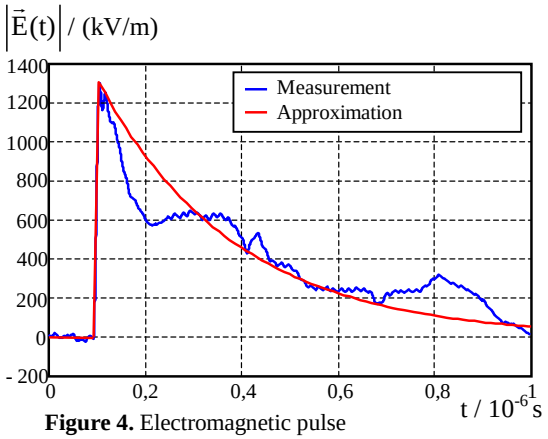

Figure 4. Electromagnetic pulse
(t_r = 7.5 ns, t_{fwhm} = 180 ns)

In this case a high field strength has to be generated to cause destruction effects on electronic circuits because the pulse is comparatively slow and has only low spectral contents in the coupling range.

If a pulse, described by these characteristics, couples into a system with the transfer function of Figure 3, the voltage on the connecting lines will have the characteristic shown in Figure 5.

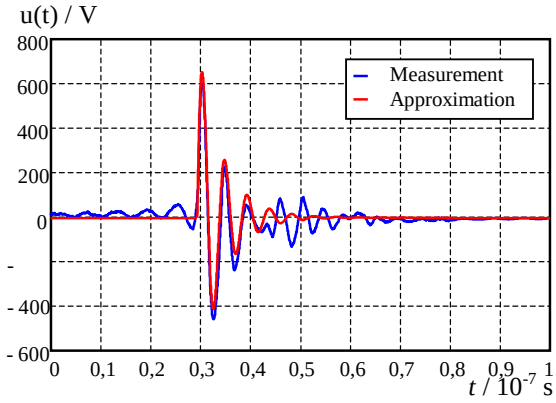

Figure 5. Electric voltage coupled into system with a line length of $l = 20$ cm

The measured signal on the connecting line can be described as a damped sinusoidal function:

$$u_k(t) = U_0 e^{-\alpha t} \sin(\omega_3 t)\,. \qquad (2)$$

In this expression α describes the damping ratio and ω_3 the angular frequency of the oscillation. $\omega_3 = 2\pi f_3$ contains the dominant coupling frequency f_3 , which is also marked in Figure 3. f_3 is dependent on the length of the connecting line, whereas α is dependent on the disturbed electronic system. The signal from Figure 5 has the following characteristics:
$\alpha = 2.1 \cdot 10^8\ s^{-1}$, $f_3 = 2.3 \cdot 10^8$ Hz and $U_0 = 821$ V
This approximation will be used as source voltage in the simulation, which will be presented later.

3. Microscopic analysis

The effects caused by the disturbances which couple into the integrated electronic devices could only be analysed by a scanning electron microscope (SEM) because of the small-sized dimensions of the integrated circuits. Two types of destruction can be observed on chip level: On the one hand one observes breakdowns because of extremely high field strengths (cp. Figure 6a) and on the other hand strip lines and bonding wires are melted because of too high current densities (cp. Figures 6b/c).
As an example for a complex integrated structure an input protection circuit of AC-/ACT-Inverters, which is completely destroyed, is shown in Figure 7.

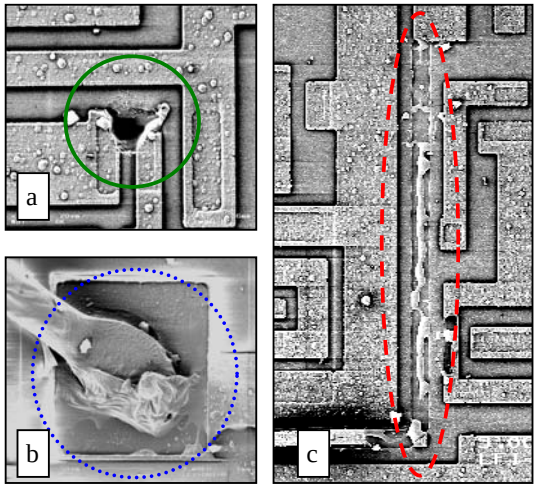

Figure 6. Destruction effects on integrated electronic devices

More details about the relations between the destruction type and the field strength of the electromagnetic pulses and the dependency of the destructions on the applied logic levels is described in other publications [4,5].

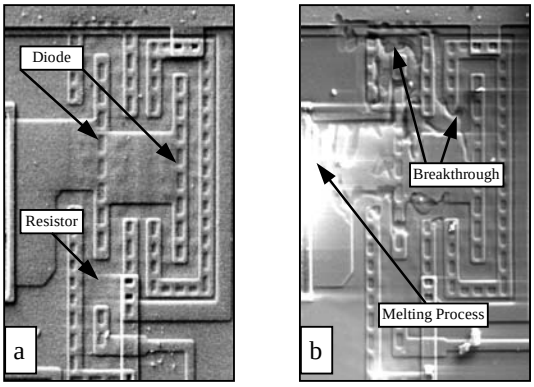

Figure 7. Input protection circuit of AC-/ACT-Inverters a) undamaged b) damaged

A scanning electron microscope (SEM) only displays the position of the destruction in a two-dimensional form. That means, that there is no

information about the depth. The SEM-image is able to show those domains of the chip, which are very susceptible. Because of the missing third dimension the analysis of detailed effects and sensitivities is limited.
It is beneficial to combine the electrostatic and the heat transfer by conduction modules. Thus it is not only possible to make a statement about the critical points in the layout but also to get informations about the time behavior of temperature and electric field strength inside the electronic devices.

4. Theory of electrothermal simulation

For the implementation of an electrothermal simulation it is necessary to connect the basic laws of electrical engineering with the basic laws of heat transfer.
This chapter gives attention to these connections and its implementation in Comsol Multiphysics.

4.1 Electromagnetic Theory

Before performing an electrothermal simulation of a process, it is necessary to decide whether all processes have to be described time-dependend or if it is sufficient to consider the electrostatic case.
The use of the electrostatic laws is allowed, if the wavelength of the fields is much larger than the dimension of the simulated structures. In Comsol Multiphysics this means, that the "electric quantity" of the simulated structure has to be smaller than 0.1 [6]. The electric quantity is the ratio of the largest dimension l_{max} of the simulated structure to the wavelength λ of the simulated fields. The analyzed logic circuit has a maximum dimension of l_{max} = 1,9 mm and is stressed by the time waveform shown in Figure 5. A maximum frequency of $f_{max} = 1 \cdot 10^{10}$ Hz results from the coupling transfer function shown in Figure 3. By that the electric quantity is:

$$\frac{l_{max}}{\lambda_{min}} = \frac{l_{max} \cdot f_{max}}{c_0} = 0{,}06\overline{3} \quad . \tag{3}$$

Consequently it is sufficient to consider the quasi-stationary case instead of implementation of the complete Maxwell equations.

For the electrostatic field the Gauß law is valid for a sufficient small volume V with $V \to 0$:

$$\frac{1}{V} \int_{Surface} \vec{D} d\vec{A} \overset{V \to 0}{=} \rho \tag{4}$$

or in differential form:

$$div\vec{D} = \rho \quad . \tag{5}$$

$\vec{D}$ describes the electric flux density and ρ the space charge density. In polarized media we can write for the polarization space charge density $\rho_p = -div\vec{P}$ and the polarization $\vec{P}$:

$$\rho - div\vec{P} = div\vec{D} \, . \tag{6}$$

By the use of $\vec{D} = \varepsilon \vec{E}$ and rearrangement of equation (6) ones receives:

$$\rho = div(\varepsilon\vec{E} + \vec{P}) \, . \tag{7}$$

As the electric field is an irrotational field we can write for $\vec{E}$:

$$rot\vec{E} = \vec{0} \, . \tag{8}$$

Therefore exists an electric potential φ which is connected with the electric field $\vec{E}$:

$$\vec{E} = -grad\,\varphi \tag{9}$$

With equation (9), equation (7) can be converted to:

$$\rho = div(-\varepsilon grad\varphi + \vec{P}) = -div(\varepsilon grad\varphi - \vec{P}) \tag{10}$$

or with help of the Nabla-operator:

$$\rho = -\nabla(\varepsilon\nabla\varphi - \vec{P}) \, . \tag{11}$$

This equation is implemented in the electrostatic modul in Comsol Multiphysics and will be used as subdomain equation.
Furthermore the equations (12a) and (12b) describe the boundary conditions for the

electromagnetic field which have to be considered additionally.

$$\vec{n}_{12} \times \left(\vec{E}_2 - \vec{E}_1\right) = \vec{0} \tag{12a}$$

$$\vec{n}_{12} \cdot \left(\vec{D}_2 - \vec{D}_1\right) = \sigma \tag{12b}$$

For regions without any area charge density σ the equation (12b) is equal to zero.

4.2 Heat transmission theory

The basis of thermal processes in different materials is the general equation of heat conduction:

$$\rho \cdot c_p \cdot \frac{\partial \vartheta}{\partial t} = div(\lambda grad\, \vartheta) + p \tag{13}$$

ρ describes the density of the material, c_p is the specific heat capacity, λ is the heat conduction coefficient, the variable ϑ is the temperature and p describes the heat source density. After transformation, the equation (13) can be expressed with help of the Nabla-operator:

$$\rho \cdot c_p \cdot \frac{\partial \vartheta}{\partial t} - \nabla(\lambda \nabla \vartheta) = p \cdot \tag{14}$$

Using the heat transmission modul in Comsol Multiphysics, this equation is implemented if we ignore convection and thermal radiation.

The combination of the electromagnetic laws from section 4.1 with the laws of heat transmission is necessary for the electrothermal simulation. The link between the modules is the heat source density p which is given in equation (14).
The heat power density is given by means of:

$$p = \vec{E}\vec{S} \,. \tag{15}$$

By the use of Ohm's law $\vec{E} = \rho \vec{S}$ and the specific electric conductivity $\kappa = 1/\rho$ follows:

$$p = \kappa \vec{E}^2 \tag{16}$$

and with help of equation (9):

$$p = \kappa(-grad\varphi)^2 \,. \tag{17}$$

By performing the gradient operation and consideration of the usual vector operations one receives:

$$p = \kappa\left(-\frac{\partial \varphi}{\partial x}\vec{e}_x - \frac{\partial \varphi}{\partial y}\vec{e}_y - \frac{\partial \varphi}{\partial z}\vec{e}_z\right)^2 = \kappa\left(\frac{\partial \varphi^2}{\partial x^2} + \frac{\partial \varphi^2}{\partial y^2} + \frac{\partial \varphi^2}{\partial z^2}\right). \tag{18}$$

The electric potential is given as a result of a simulation in the electrostatic modul in Comsol Multiphysics. The heat power density p, which is described in equation (18), can be used as the heat source density in equation (14).

5. Electrothermal Simulation

According to section 3 there are two different kinds of destruction on semiconductor chips caused by electromagnetic pulses. In this section one example of each of the destruction effects will be shown and discussed.

5.1 Simulation of breakthroughs

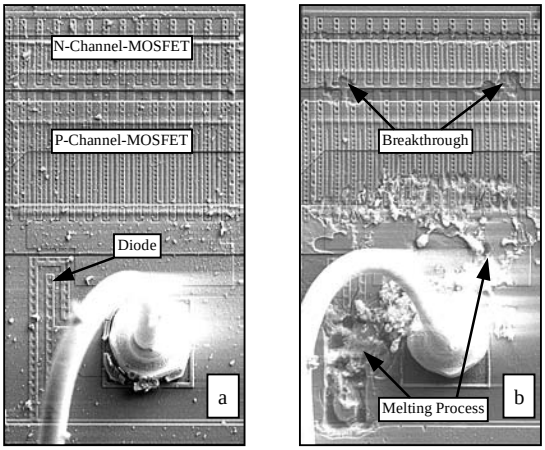

Figure 8. Last transistor stage and output circuit of AC-/ACT-Inverters

In Figure 8 the last transistor stage and the output circuit of an ACT CMOS Inverter is shown. After impact of an electromagnetic pulse

with a maximum amplitude of 1290 kV/m one recognizes breakthroughs inside the transistors (cp. Figure 8b). The position of the destruction on the chip is located in an area where many different structures of many different materials are on top of each other. In order to analyse the specific processes, the p-channel-MOSFET, shown in Figure 8, is simulated.

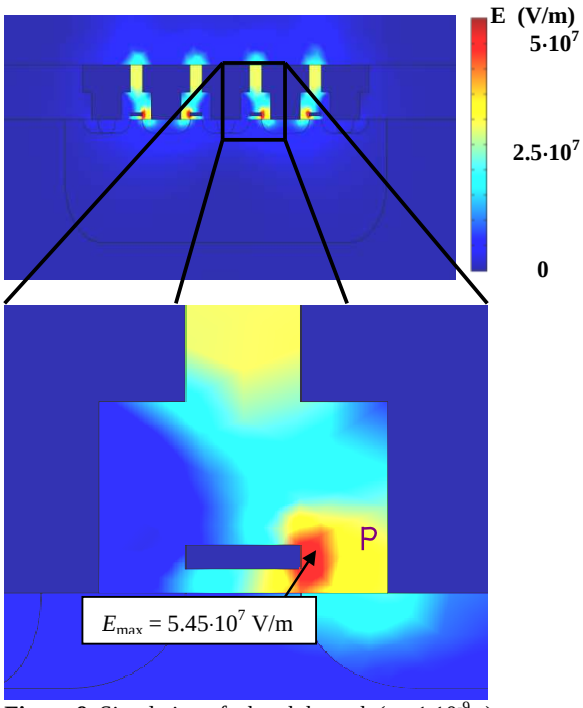

Figure 9. Simulation of a breakthrough ($t = 1 \cdot 10^{-9}$ s)

Additionally to the normal electric potentials in active system state of the device the analytical description of the coupled disturbing signal (cp. equation 2) is impressed on the drain contact. The maximum field strength occurs at point P at the time $t = 1 \cdot 10^{-9}$ s as shown in Figure 9.

The point of maximum field strength is located in silicon, which has a breakdown field strength of $E_{br} = 2 \cdot 10^7$ V/m. This area is embedded in silicon dioxide, characterized by a breakdown field strength of $E_{br} = 1 \cdot 10^8$ V/m. The time of breakdown $t_{br} = 0.25 \cdot 10^{-9}$ s can be determined from the time behavior of E_x, which is shown in Figure 10.

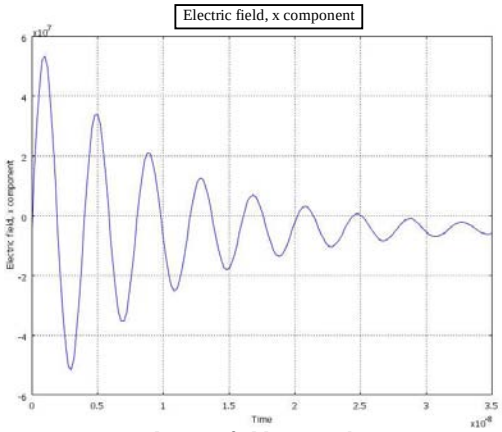

Figure 10. Electric field strength E_x at point P (E_{EMP} = 1290 kV/m)

5.2 Simulation of melting processes

Analog to the simulation of the breakdown effects it is possible to simulate the melting processes on the devices. In order to simulate these processes it is necessary to interconnect the electrostatic and heat transfer modules as presented in section 4. In order to guarantee the heat flux in all directions it is recommended to carry out the thermal simulation in a 3D-model.

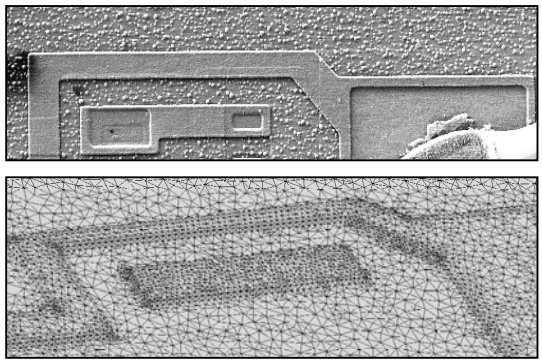

Figure 11. SEM-photo and model of an input circuit

As an example, an input circuit of a gate and its corresponding model is shown in Figure 11. During impact of an EMP with a field strength of 1000 kV/m it comes to a melting process at the narrowing of the pcb track (cp. Figure 12a).

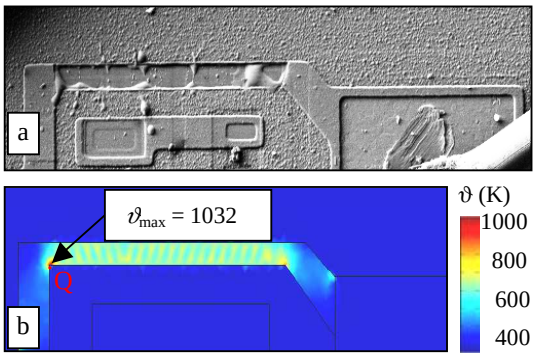

Figure 12. Simulation of a melting process of a pcb track **($t = 6 \cdot 10^{-9}$ s)**

The simulation in Figure 12b shows an increase of the temperature above the whole length of the restriction. The maximum temperature of ϑ_{max} = 1032 K can be observed at time t = 6 ns in point Q. By analysing the time behavior of the temperature, we are able to identify the time when the melting temperature of the pcb track is exceeded. In Figure 13a it is observable, that the melting process ($\vartheta_{melting}$ = 933 K) starts at $t_{melting}$ = 3.5 ns.

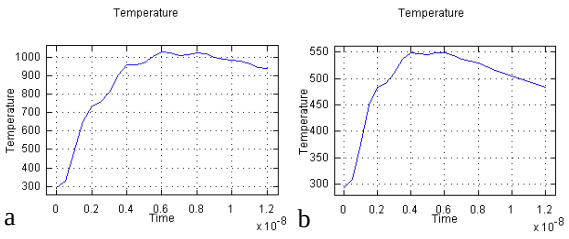

Figure 13. Temperature at point Q in Figure 12.
a) E = 1000 kV/m; b) E = 650 kV/m

The non-destructed case is shown in Figure 13b. The temperature remains below the critical melting temperature.

6. Conclusions

The investigation of the destructionon effects on logic devices during impact of fast transient electromagnetic pulses is only possible by later SEM microscopy. There are no informations about the times of destruction. It is possible to locate and classificate the destruction effects on chip level by SEM but it only displays the position of the destruction in a two-dimensional form. That means, there is no information about the destruction in depth.

By the use of simulations it is possible to get these informations. The structure of the integrated circuits could be modeled in all three dimensions. By the combined use of the electrostatic and the heat transfer modules, it is possible to impress a disturbing signal and get informations about the time behavior of the electric field strength and temperature.

Because the models are very complex it is only possible to simulate a part of the whole structure of the integrated circuits. Although, the use of simulations gives the possibility to get more informations about the field strength and temperature distribution in the complex structure on chip level. Important parameters like the time of destruction and the exact position of the most vulnerable structures can be obtained.

8. References

1. S. Korte, *Empfindlichkeit elektronischer Schaltungen gegenüber transienten Störgrößen*, Diploma thesis, University of Hannover (2004)
2. C.D. Taylor, D.V. Giri, *High Power Microwave Systems and Effects*, Taylor and Francis, Oxford (1994)
3. M. Camp, *Empfindlichkeit elektronischer Schaltungen gegen transiente elektromagnetische Feldimpulse*, Ph. D. thesis, Shaker Verlag, Aachen (2004)
4. M. Camp, S. Korte, H. Garbe, *Classification of the Destruction Effects in CMOS-Devices after Impact of fast Transient Electromagnetic Pulses*, EUROEM 2004 BoA, Magdeburg 2004
5. M.Camp, H.Garbe, D.Nitsch, *Influence of the Technology on the Destruction Effects of Semiconductors by Impact of EMP and UWB Pulses*, Proceedings of 2002 IEEE International Symposium on Electromagnetic Compatibility, pp. 87-92, Minneapolis, USA (2002)
6. COMSOL AB, *Users Guide, FEMLAB: Electromagnetics*, Stockholm (2000)